Deep-sea temperate-tropical faunal transition across uniform environmental gradients

Timothy D. O'Hara [a,1], Alan Williams [b], Skipton N.C. Woolley [b], Amy W. Nau [b], and Nicholas J. Bax [b,c]

[a] Museums Victoria, GPO Box 666, Melbourne, VIC 3001, Australia

[b] CSIRO Oceans and Atmosphere, Castray Esplanade, Hobart, TAS 7001 Australia

[c] Institute for Marine and Antarctic Science, University of Tasmania, Hobart, TAS 7001, Australia

[1] To whom correspondence should be addressed. Email: tohara@museum.vic.gov.au

Abstract

The biogeography of the deep-sea benthic fauna is uncertain due to the vast size and incomplete exploration of these environments. While shallow water assemblages are differentiated into tropical, temperate and polar faunas, it is unknown whether these units extend to lower depths. Here we use model-based statistics to analyse megafaunal benthic samples along a 2,300 km transect off the eastern Australian continental margin. We show that a temperate-tropical transition between 33-31˚S occurs at both lower bathyal (~2500 m) and abyssal (~4000 m) depths. This transition occurs despite almost uniform temperature, salinity and dissolved oxygen concentrations occurring across latitudes at these depths. Conversely, the patterns are consistent with the flux of organic matter to the seafloor, which varies from being relatively high in the productive temperate off SE Australia to low levels in more-oligotrophic tropical waters. Biodiversity is not uniform across the deep-sea and regional-scale heterogeneity needs to be incorporated into marine park designs.

Keywords

Megafauna, benthos, Tasman Sea, Australia, continental margins, abyss

1. Introduction

Deep-sea ecosystems are one of the world's major ecological research frontiers, giving us new perspectives on macro-ecological questions (Danovaro *et al.*, 2014). The deep sea (below 200 m) is the third biological realm after terrestrial and shallow marine systems, and is characterised by very cold water, extreme pressure, little to no light and limited food, with organic matter residues sinking from surface waters or transported down continental margins. However, our knowledge of large-scale spatial patterns at lower bathyal and abyssal depths (2000-6500 m) is limited, because of the logistical difficulty in sampling the vast extent of this biome (the largest on the planet).

Patterns of species distributions are well known for shallow water (0-200 m) marine environments. Here studies have shown marked compositional changes between tropical, temperate and polar assemblages (Ekman, 1953). These patterns were recognised as early as the 1850s, when Edward Forbes composed a global map showing marine life (fish, molluscs, echinoderms and cnidarians) distributed in latitudinal bands or “homoiozoic belts” (Johnston, 1856). These assemblages have formed in the context of a cooling of the earth since the mid Eocene (56 my) which steepened the temperate gradient from equator to pole, creating new niches at temperate and polar latitudes, and the evolution of distinct faunal assemblages (e.g. Crame, 2018; Fine, 2015; O'Hara *et al.*, 2019). The boundaries between these bands are not sharp however, in the southern hemisphere, the temperate-tropical transition gradually occurs between 30-40°S and the temperate polar transition between 50-60°S (O'Hara *et al.*, 2011).

Regional evidence suggests that upper to mid bathyal faunas (200-2000 m) are also structured into broad polar, temperate and tropical bands (O'Hara *et al.*, 2011). This may reflect latitudinal variation in temperature (particularly at upper bathyal depths) or other oceanographic variables such as carbon flux (Watling *et al.*, 2013; Woolley *et al.*, 2016). However, at mid bathyal depths (~2000 m) the connection between faunal composition and oceanographic gradients is less obvious, although broad polar, temperate and tropical faunal bands persist. O’Hara *et al.* (2011) found that only 6% of ophiuroid species were shared between tropical New Caledonia and temperate southern New Zealand at 1200-2000 m, despite there being only minor differences in environmental variables. The palaeontological record for bathyal faunas are generally too fragmentary to be biogeographically informative (Thuy *et al.*, 2012).

Global abyssal biogeography began with the zoological summary of the HMS Challenger expedition (1872-6). Murray (1895) documented the widespread distributions of the abyssal fauna but found few animals were truly cosmopolitan, i.e. there was some biogeographic structure to abyssal faunas. Vinogradova (1959) and Menzies et al. (1973) produced the first global biogeographic maps of the abyssal fauna based around oceanic basins separated by the newly discovered mid-ocean ridges. However, the biological data were still fragmentary and there were concerns that apparent basin-scale endemism was an artefact of inadequate sampling (Madsen, 1961). However, the emerging consensus was that the abyssal faunas of the Southern, Atlantic, West Pacific and East Pacific Oceans could be distinguished, although with less differentiation than more shallow water faunas. The distinctiveness and relationships of the western Indian Ocean and Arctic faunas were disputed (Madsen, 1961; Menzies *et al.*, 1973). The Global Open Oceans and Deep Seabed (GOODS) Biogeographic Classification (UNESCO, 2009) and a recent update (Watling *et al.*, 2013) further divided these oceanic faunas using south-north gradients of the environmental surrogates: temperature, oxygen and phytoplankton production.

The position of the northern boundary of the abyssal Southern Ocean fauna (the polar to temperate/tropical transition) has varied between these analyses. Vinogradova (1959) placed it around ~40°S, Menzies *et al.* (1973) at ~10°N, the GOODS classification at the oceanographic Antarctic Convergence (~55°S) and Watling *et al.* (2013) followed the elevated bathymetry of southern Indian and Pacific tectonic ridges, which meander between 30-65°S.

A separate tropical to temperate abyssal transition has been less emphasised, particularly in the southern hemisphere, where the abyssal fauna at temperate latitudes has generally been considered to be continuous with either the Southern Ocean fauna (Menzies *et al.*, 1973) or central Indian/Pacific/Atlantic faunas (UNESCO, 2009; Vinogradova, 1959; Watling *et al.*, 2013). The GOODS classification did distinguish a Central Pacific province (10°S to 10°N) based on productivity data, however, this was reduced to a funnel-shaped province in the eastern Pacific by Watling et al. (2013) to more accurately reflect areas of enhanced sea surface productivity from equatorial upwelling.

A 2017 voyage of the RV 'Investigator', to survey the deep-sea benthic fauna in newly created marine parks off Australia's eastern continental margin (42-23°S), provided the opportunity to test for the existence of a tropical-temperate faunal transition at lower bathyal (~2500 m) and abyssal (~4000 m) depths. Specifically we investigated whether these lower bathyal or abyssal faunas exhibited latitudinal turnover similar to that found at shallow to mid slope depths (0-2000 m) (O'Hara *et al.*, 2011) or whether the faunas are more or less uniformly distributed throughout this study region along the lines predicted by modern maps of abyssal biogeography (UNESCO, 2009; Watling *et al.*, 2013). The question can be reformulated as: how deep does the temperate-tropical faunal transition extend?

2. Materials and Methods

2.1. Study area geology and oceanography

The Tasman Sea was formed through the tectonic rifting of Australian and New Zealand continental masses (Gaina *et al.*, 1998). A rift valley along the eastern Australian margin formed approximately 90 Mya. Separation started south of Tasmania 84 Mya and gradually proceeded northward until spreading stopped approximately 52 Mya. The result was the triangle-shaped abyssal Tasman Basin, flanked on the west by the Australian margin, on the east by the Lord Howe Rise (made up of several conjoined continental fragments) and open to the Southern Ocean in the south (Gaina *et al.*, 1998). The northern basin apex occurs at 24°S, with the Cato Trough forming a relatively shallow (3400-3500 m) narrow (~10 km wide) channel to the north between the Marion and Chesterfield plateaux (Keene *et al.*, 2008). The abyssal Tasman seafloor was generated along a now extinct spreading ridge running south to north (Gaina *et al.*, 1998). However, the main volcanic feature of the basin is now the offshore Tasmantid chain of seamounts, created by the Australian plate moving over a weak crustal hotspot from 33.2 ± 1.5 Mya (Wreck Seamount, 22.2°S) to 6.5 ± 0.6 Mya (Gascoyne Seamount, 36.6°S) (Crossingham *et al.*, 2017).

The continental slope along eastern Australia is broadly convex from the shelf break down to 1500 m, then concave until 3000 m, before forming a steep rocky scarp down to the abyssal plain at 4500-5000 m (Keene *et al.*, 2008). There is little continental rise present and siltation fans from rivers are small (Keene *et al.*, 2008). However, sediment from terrestrial and pelagic sources does accumulate on the upper margin, and can be transported downslope along the numerous submarine canyons (Heap and Harris, 2008), via slumping due to slope failure (Hubble *et al.*, 2012) or from particularly productive continental shelves at the northern end of the Tasman Sea (Keene *et al.*, 2008). Bottom currents can create large elongate drift mounds on the abyssal plain (Keene *et al.*, 2008).

Water currents are modified by the topography of the Tasman Basin. Antarctic Bottom Water (ABW) arrives at abyssal depths from the south-west. The enclosed northern end of the Tasman Basin below 3300 m forces the current into clockwise eddies (Tilburg *et al.*, 2001) with a return flow south along the Lord Howe Rise (Condie, 1994). These abyssal eddies cause upwelling near Fraser Island (Keene *et al.*, 2008), and can modify the course of the eastern Australian current at the surface (Tilburg *et al.*, 2001). The strong northward flow along the Australian margin removes sediment from the lower continental slope leaving a rocky surface, forming shallow (20-50 m deep) moats in the abyssal plain at the base of the margin, and possibly undermining sediment layers further up the slope, causing slumping (Hubble *et al.*, 2012; Keene *et al.*, 2008). Moving up the water column, North Atlantic Deep Water (NADW) is present at 2500 m, originating in the North Atlantic Ocean, upwelling into the southern Atlantic, moving east across the Indian Ocean with circumpolar currents, before also entering the Tasman Sea from the south-west (Tomczak and Godfrey, 2003). Antarctic Intermediate Water (AAIW) is present around 1000 m which is formed at subantarctic latitudes in the Southern Ocean. However, it enters the Tasman Sea from two directions, one flowing from the south-west and the other from the north and east, the latter having become entrained by the counter-clockwise equatorial gyre in the southern Pacific (Tomczak and Godfrey, 2003). Surface currents arrive from north in the form of the East Australian Current (EAC). Most of the surface current turns east from the Australian margin at 32-35°S, although deeper flows and eddies move south as far as Tasmania (Ridgway and Dunn, 2003).

The temperature, salinity and oxygen properties of the deeper water masses differ little over the latitudinal range of this study (Fig. 1). The CARS2009 dataset (Ridgway *et al.*, 2002) indicates that water temperatures rise slowly from 4000 m (1.1°C), through 2500 m (1.9°C) to 1000 m (5.0°C), salinity is very similar at both 4000 and 2500 m (34.72‰), and slightly less at 1000 m (34.47), oxygen levels are slightly higher at 4000 m (4.49 ml/l) compared to 2500 m (4.13) and 1000 m (4.06) (see Supplementary Information). There are no hypoxic (O_2 <1.7 ml/l) or anoxic (<0.02) oxygen minimum zones within the study region (Falkowski *et al.*, 2011).

Net primary production (NPP) is greatest (>700 g C_{org} m^{-2} d^{-1}) at temperate latitudes (48-38°S) across southern Australia (Fig. 1; Behrenfeld *et al.*, 2006). Offshore from coastal waters, NPP steadily declines with lower latitudes, becoming relatively oligotrophic (300 mg C m^{-2} d^{-1}) north of the Tasman Front (31°S). The Seasonal Variation Index (SVI), the standard deviation over the mean of NPP, is also elevated at temperate latitudes, particularly south of Tasmania (Lutz *et al.*, 2007). Phytoplankton communities over the continental margin vary from small to large diatoms typical of the temperate neritic regions to tropical oceanic dinoflagellates off the Queensland coast (Hallegraeff *et al.*, 2017). Much marine productivity is recycled (consumed) at shallow water depths, and carbon that arrives on the abyssal seafloor is 2-3 orders of magnitude less than is present in surface waters (Lutz *et al.*, 2002). The slope seafloor is well oxygenated and bioturbation is abundant, although the carbon content of the sediments is less than 1% (Keene *et al.*, 2008), which is poor by global standards (Seiter *et al.*, 2004). The composition of the sediments is depth-dependent, with mixed terrestrial siliceous and biogenic carbonate sediments dominating the shelf and upper slope, gradually changing to finer pelagic-derived sediments (mainly coccolith and foraminifera remains) with depth (Keene *et al.*, 2008). In the Tasman Sea, the lysocline occurs at

~3,600 m (Martinez, 1994), below which carbonate skeletons start to dissolve and the sediments become very fine ooze.

2.2. Samples

The study design was to deploy a beam trawl (4 m metal beam) to collect samples on soft sediment substrata at the target seafloor depths of 1000, 2500 and 4000 m at every 1.5 degrees of latitude along the western boundary of the Tasman Sea from 42° to 23°S, traversing seven Australian Marine Parks (AMPs) (Fig. 2). Each site was mapped (bathymetry and backscatter) prior to deployment using a Kongsberg EM 122 12kHz multibeam sonar. Environmental data (temperature, salinity, pressure) were collected by a Sea-Bird SBE37SM sensor.

Beam trawl samples were sorted, weighed and preserved (95% ethanol) on-board into broad taxonomic groups (Table S1, S2), and sent to taxonomic experts for identification. The following groups of megafauna were subsequently identified to operational taxonomic units (mostly to species, some to genus or family), counted and used as the basis of subsequent statistical analyses: sponges, anemones, octocorals, barnacles, decapods, pycnogonids, annelids, echinoderms, gastropods, bivalves, cephalopods and fish (see acknowledgements).

2.3. Statistical analyses

All analyses were performed using the R statistical environment v 3.4.3 (R Core Team, 2017) and code scripts are provided in the supplementary information (S3). Exploratory analyses of the data were performed using non-metric multivariate statistics (Clarke and Warwick, 2001). Species included in analyses were restricted to those that occurred in at least 4 samples (Table S4). The species-site abundance data was log(x+1) transformed to down-weight the influence of abundant taxa. A triangular dissimilarity matrix was created using the Bray-Curtis coefficient with the function vegdist(method="bray") function in the 'vegan' v2.4.5 package (Oksanen *et al.*, 2016). Hierarchical clustering of sites was performed using hclust() in the base R 'stats' package and non-metric multidimensional scaling (nMDS) ordination by metaMDS() also in the 'vegan' package. The SIMPER method of identifying species that discriminate between groups (available in 'vegan') was not used, as this method does not adequately describe mean-variance relationships in multivariate data (Warton *et al.*, 2012). Beta-diversity was computed between each cluster using the Sorenson coefficient, and then decomposed into compositional (Simpsons) and richness (SNE) components using the methods of Baselga (2010) as implemented by the beta.pair() function in the betapart R library (Baselga *et al.*, 2018).

We used a model-based approach for the analysis of community data as this allowed for the direct specification of a statistical model, which correctly describes mean-variance relationships and allows for an estimate of uncertainty in the resulting predictions (Warton *et al.*, 2015). We used Species Archetype Models (SAMs; SpeciesMix R package v0.3.4) (Dunstan *et al.*, 2011; Dunstan *et al.*, 2013) to determine whether distinct species-groups existed at tropical and temperate latitudes across the study depth range. SAMs group species into 'archetypes' based on species' shared responses to environmental or geographic (covariates in the model) data. For our study, we fitted SAM with a negative binomial error distribution. This model contained species-specific independent intercepts, which help to capture the differences in the underlying species abundance independently of covariate effects (Dunstan *et al.*, 2013). The model enabled us to correctly model the error distribution of count data derived from the beam trawl catches while also estimating the mean species-specific density across all sites. This helped to reduce artefacts in the grouping of 'rare' and/or 'common' species into archetypes based on their density. One characteristic of SAMs is the number of groups estimated by the model is unknown (latent) (Dunstan *et al.*, 2011). Crucially, the optimal number of distinct archetypes can be determined based on the model likelihood using the Bayesian Information Criterion (BIC). The fitted Generalised Linear Model (GLM) associated with each archetype can then be used to predict its density across the study extent. A hard classification of archetypes can be generated by assigning the archetype with the highest predictive value to each pixel.

For the SAMs analysis, we restricted species to those that occurred in four or more samples, and explored the potential utility of a range of environmental variables: depth and latitude (derived from sample means), annual mean temperature, salinity and oxygen (ml l^{-1}) (from CARS2009), and mean annual net primary productivity (NPP, g C m−2 year−1), seasonal variation of net primary productivity (SVI, g C m−2 year−1; SVI) and carbon flux to the seafloor (POC flux, g C m−2 year−1) (Table S5). NPP and SVI were generated from a vertically generalized production model (VGPM) (Behrenfeld and Falkowski, 1997) from satellite-derived chlorophyll (SeaWiFS) data from the years 2003 to 2010 (see http://www.science.oregonstate.edu/ocean.productivity/). POC flux was estimated using NPP and SVI data and a productivity export model (Lutz *et al.*, 2007). We used 1st and 2nd degree orthogonal polynomials of the explanatory variables. The area sampled per site was included as an offset in the model. The offset is included into the model on the log-scale to match the linear predictor, which is also on the log-scale for a negative binomial model. This had two benefits, accounting for unequal sampling at each site and preserving the data as counts (O'Hara and

Kotze, 2010). We used six random initialisations of an Expectation Conditional Maximisation (ECM) algorithm (encoded in the SpeciesMix package) to find good starting values for each SAM model fit. Within each model fit, starting values from the ECM are maximised using Newton-Raphson optimisation of the model log-likelihood (Dunstan *et al.*, 2013). We determined the optimum number of archetype groupings (ranging from 2 to 10) based on BIC. Explanatory variables for predictions were transformed via a linear fit to the orthogonal polynomials from the selected SAMs model and the mean of sample-area was used as the offset. Archetype responses to each environmental variable were generated by setting all other variables to their mean values before prediction (Dunstan *et al.*, 2013). The probability of species belonging to a given archetype was determined from posterior archetype membership (tau) enabling us to understand which species are predicted to belong to each group once they have been estimated (Dunstan *et al.*, 2011). Predictions were made across a latitude (degree increments) x depth (500 m increments) grid.

3. Results

The multibeam sonar revealed a continental slope topography that was much more complex and rugged than expected, with the margin incised by numerous canyons, sediment slumps, cliffs and other areas of exposed rock (Fig. 3). Consequently, the location, depth and swept area of each sample varied considerably from the original target due to the need to find relatively flat areas of mostly soft sediment (Table 1). In addition, a number of 1000 m beam trawls at the southern end of the transect were abandoned due to operational difficulties, however we retained the remaining southern 1000 m site (013) as it was informative, particularly in the multivariate analysis (in the model based analysis it appears to be species poor due to the restriction of species to those that occurred in 4 or more samples). Our sampled environmental data was highly correlated (Pearson $R=0.993$, $p<0.001$) with modelled oceanographic data of the global CARS2009 dataset.

After adjustment for trawled area, total specimen weight and density varied substantially between samples (Table 1). The highest biomass occurred at 2785 m in the Freycinet AMP (sample 004), which was dominated by many holothurians (*Benthodytes* sp, *Molpadiodemas* sp and *Pseudostichopus peripatus*). Sample 022, from a similar depth but softer substrata, was also characterised by high biomass (of holothurians) and high density (ophiuroids). Sample 080 from 1225 m included a decaying manta ray with associated scavengers and predators. Sample 100 included a dead pilot whale skull and vertebrae which hosted *Idas* bivalves and *Osedax* worms (not previously reported from Australia). These specialist animals occurred at only one site and thus were not in included in our analyses. All samples from around 4000 m were characterised by relatively low biomass and abundance.

The number of identified taxa was 881, with 432 occurring in 2 or more samples, and 184 in 4 or more samples (Table S6). Of these taxa, only 387 could be assigned a species-level scientific name, indicating that potentially up to 56 % of the fauna is new to science. The most widespread species from 19 samples, was an undescribed ampharetid polychaete (sp. C). The species-sample matrix is included in the Supplementary Information (Table S4).

The MDS ordination was geographically interpretable when overlayed by 6 groups defined from the hierarchical cluster analysis (Fig. 4), which essentially divided the samples into temperate (southern) and tropical (northern) groups across each of the targeted depth strata (groups herein designated as S1000, N1000, S2500, N2500, S4000 and N4000). Within group patterns did not necessarily reflect a latitudinal gradient, although neighbouring samples frequently clustered together. Our failure to obtain all our targeted southern samples at 1000 m precluded establishing the temperate-tropical transition at this depth for this data, although the sample from Hunter AMP (069, 32.5°S) was closely associated with the N1000 group. At ~2500 m, two samples, off Newcastle (067, 33°S) and Hunter AMP (070) were intermediate between S2500 and N2500 clusters on the MDS plot, although they were included in the temperate group on the cluster dendrogram. At 4000 m, the Hunter sample clustered with the S4000 group, which was distinctly separated from N4000 samples. Thus the data is consistent with a temperate-tropical transition between 33 and 30°S that extends down to abyssal depths (>3500 m). The Sorensen Beta-diversity indices between these clusters reflect differences in composition more than species richness, except for relatively species poor clusters S1000 and N4000 (Table S7).

In the Species Archetype Model analysis, the model fitted to quadratic transformations of depth and latitude resulted in the lowest BIC (12420) for any combination of two environmental parameters (using linear or quadratic terms, and excluding longitude which was highly correlated with latitude, Pearson r=0.95). Adding extra parameters resulted in very little decrease in BIC (Table S8). Many of the other environmental parameters were also correlated with these vertical and horizontal spatial parameters (Table S9), including temperature (Pearson r=-0.90), salinity (0.77) and oxygen (0.87) with depth, and NPP (-0.98) and SVI (0.65) with latitude. Our formula for POC flux to the seafloor incorporates terms for depth, NPP and SVI and so is correlated with both depth (0.68) and latitude

(0.35). Models with any of these terms resulted in higher BIC. The best model that excluded depth/latitude included quadratic terms for temperature and POC flux (BIC=12569).

Once we decided on the parameters, we identified the optimal number of groups as five (Fig. 5a). If we selected more than five archetype groups, at least one of these extra groups had relatively few species or the predicted density was very low, which suggested an overfitting of the data. The predicted distribution of the five archetypes were interpretable on a grid of latitude and depth (Fig. 5b-e). A single archetype was predicted to occur at relatively high densities across the entire study area at 1000 m (Fig. 5d), although the highest values occurred at northern latitudes (N1000, Fig. 5e). The failure to predict an S1000 group is not surprising given there was only one sample and the analysis was restricted to species that occurred in 4 or more samples. Separate temperate and tropical archetypes were predicted to occur at both 2500 and 4000 m with the transition occurring between 33 and 31°S, although the predictions for each archetype (Fig. 5e) indicate that compositional turnover is likely to be gradual between 35 and 30°S. Standard errors (Fig. S10) were greatest for each archetype around the areas with highest predicted densities, indicating high variation in species abundances between samples. The archetype fit to the spatial prediction points was also graphed against POC flux and temperature (Fig. S11).

The 184 taxa in the SAMs were assigned to the five archetypes as follows (Table S12): N1000 (15%), S2500 (30%), N2500 (19%), S4000 (28%), and N4000 (9%), i.e. at 2500 m, three times the number of taxa were assigned to the southern than northern groups, and at 4000 m, 1.5 times as many. However, these southern/northern archetypes were compositionally distinct and did not merely reflect differences in species richness. Only 25% of species were predicted to occur in more than one archetype with tau values of > 0.05, including only 2 out of the 16 species (12%) in the N4000 archetype. Nor was this an artefact of the limited sampling. Examination of the known distribution of the N4000 species (Table S13) indicated that half these species were longitudinally widespread but restricted to tropical latitudes (< 35°). For example, the Faceless Cusk Fish (*Typhlonus nasus*, Fig. 3d) occurs at abyssal depths throughout the tropical Pacific and Indian Oceans.

4. Discussion

We found turnover of benthic deep-water species along the Australian continental margin with both depth and latitude. Samples from around 1000 m, 2500 m and 4000 m differed considerably in community composition and species richness with depth, conforming to well-known bathymetric patterns (Carney, 2005; Woolley *et al.*, 2016). Interestingly, depth was a superior predictor of community composition than oceanographic variables that are known to vary with depth, such as temperature, salinity and oxygen. There was as much or more turnover in community and richness between 2500 and 4000 m as there was between 1000 and 2500 m, despite there being less environmental change (S5, S7). We did not have enough samples to model more complex non-parametric relationships between environmental variables and community composition.

There was a clear temperate-tropical transition across our study region at lower bathyal and abyssal (LBA) depths (>2000 m). The groups of temperate and tropical species were drawn from across the faunal taxonomic spectrum from fish to sponges. The transition was roughly congruent between our targeted depth layers despite the large turnover of species that also occurs with depth. Although, we did not have enough data to conclusively distinguish a temperate and tropical fauna at 1000 m, earlier spatial analyses of upper (200-2000 m) continental slope data from this region have found distinct faunas in these biomes for ophiuroids (O'Hara *et al.*, 2011), squat lobsters (Schnabel *et al.*, 2011) and demersal fish (Last *et al.*, 2010). LBA regional species richness is known to be elevated at temperate latitudes in at least one dominant group: ophiuroids (Woolley *et al.*, 2016). However, the groups identified here were not solely an artefact of differing species richness, one species group being a subset of the other. Our transitions represent assemblage compositional changes across latitude and depth.

Cluster and model-based analyses placed the latitudinal transition at slightly different latitudes, 33-30°S and 35-33°S respectively. The fine-resolution (0.04 degree) analysis of O'Hara et al. (2011) put the boundary of the 200-2000 m ophiuroid fauna just north of 30°S. However, this apparent sharp boundary was an artefact of the clustering algorithm and O'Hara et al. (2011) found that mapping species range limits showed a more gradual turnover in the upper bathyal fauna between 40 and 30°S. The individual archetype predictions in Fig. 5e show a similar pattern for these data; there is considerable overlap around the transition boundary, particularly at 2500 m. Nevertheless, patterns of beta-diversity (or distance-decay relationship) have been found to be not uniform along latitudinal gradients, with alternating latitudinal bands and transition zones (O'Hara *et al.*, 2011).

Our temperate-tropical transition was broadly congruent with that found by Vinogradova (1959), who separated Indo-Pacific and Southern Ocean abyssal faunas at around 40°S. However, pre-1960 sampling around this latitude was sparse and thus her placement of the boundary was approximate. Conversely, our results do not support the abyssal biogeographic schemes of Menzies et al. (Menzies *et al.*, 1973) or Watling et al. (2013), who both recognised a very broad 'Austro-Indian Antarctic' area based on temperature and topology, which extended from the Antarctic ridge (~60°S) to the northern apex of the Tasman Sea (23°S). Thus our results were more consistent with previous biogeographies produced from quantitative analyses of biological samples (Vinogradova) rather than environmental factors (Menzies, Watling). This underscores our finding that there is a horizontal temperate-tropical transition at 2500-4000 m depths that is not associated with a corresponding change in water temperature, salinity or oxygen (Table 1, S5). The major role of temperature in defining horizontal species range limits hypothesised to occur in shallow water (Stuart-Smith *et al.*, 2017) does not appear to hold for the tropical-temperate benthic LBA fauna.

The transition does not seem to be related to geology either. Maps of geomorphic units (e.g. knoll, terrace, slope, rise, plateau) do show considerable diversity along the Australian eastern margin (Heap and Harris, 2008), however, it is unclear whether many of these large-scale units has any direct influence on seafloor faunal composition, apart from where they provide distinctly different habitats at fine scales by altering bottom water flows or the relative extent of exposed rock and soft sediment (Williams *et al.*, 2009). A regional change in substratum composition can generate biogeographic discontinuities (e.g. Hidas *et al.*, 2007). Previous studies indicate that local topography and seafloor characteristics show greater importance at finer scales, while oceanographic properties have greater explanatory power for larger-scale patterns, at least on the continental shelf and slope (Williams *et al.*, 2010), consistent with the proposed hierarchical structuring of Australian biogeography more generally (Last *et al.*, 2010).

One oceanographic variable that did form a latitudinal gradient at the seafloor is net primary production (Table 1), which is dependent on in surface waters and depth (Fig. 2) (Lutz *et al.*, 2007). Primary production was both greater and more seasonal near Tasmania and Bass Strait, driven by upwelling of nutrients in spring and to a lesser extent autumn. Seasonal pulses of production increase carbon flux to deep water (Lutz *et al.*, 2007) with nutritious sinking aggregates ('marine snow') often visible on the seafloor (Gage and Tyler, 1991). Larger zooplankton such as salps can swarm in productive conditions, further enhancing carbon flux to the seafloor through the sinking of faeces and carcasses (Henschke *et al.*, 2016). Offshore waters north of 30°S were more oligotrophic and less seasonal, in line with much of the tropical ocean except the continental shelves. Increased water temperatures are known also to reduce mixing of surface and deeper waters further decreasing export to the seafloor (Henson *et al.*, 2009). It is not just the quantity of organic matter that differs but the composition as well. The species of mega-fauna (e.g. whales and sharks/rays) that fall as carcases to the seafloor, important to deep-sea trophic systems (Gage and Tyler, 1991;

Smith and Baco, 2003), will differ between different regions. There are different plankton communities in temperate (large diatoms) and tropical (dinoflagellates) regions (Hallegraeff *et al.*, 2017; Raes *et al.*, 2018) that may require specialised physiologies or bacterial intermediates (e.g. symbionts) for benthic animals to be able to exploit them. There has been a shift to diatom-based food webs around Antarctica over the last 15 my in response to cooling events (Crame, 2018). There is evidence that variation in carbon flux to the seafloor can drive differences in both species richness and composition at local scales (Smith *et al.*, 2009; Wolff *et al.*, 2011) and species richness at regional scales (Woolley *et al.*, 2016). Various authors have speculated about the biogeographic implications of carbon flux variability on abyssal faunal composition (Watling *et al.*, 2013) but we are unaware of any previous studies that have quantified this relationship at large spatial scales.

Extant biogeographical patterns will be also influenced by the history of the biota. The composition and diversity of regional faunas are determined by speciation, extinction and migration over evolutionary timescales (MacArthur and Wilson, 1967). However, the biogeographic boundaries seen today need to be maintained by ecological or neutral processes that prevent homogenisation of regional faunas. These processes can include environmental thresholds, biotic interactions or dispersal limitations (Wiens and Donoghue, 2004). The interaction of water currents and topology can create biogeographic boundaries by creating long-term barriers to dispersal, i.e. species are prevented from dispersing from their ancestral range to all their potential habitat. Offshore surface waters In the Tasman Sea (East Australian Current) flow from north to south as part of the Southern Pacific gyre. At 1000 m, some Antarctic Intermediate water originating in the SE Pacific also flows in this direction but some originates from the south (Chiswell *et al.*, 2015). In deeper waters, water inflow is from the south-east, pushed along by circumpolar currents in the Southern Ocean. At 4000 m, the Tasman Basin is enclosed at the northern end (Fig. 2). Consequently, bottom water forms a cyclonic system that flows north along the Australian margin, before forming eddies and turning south along the Lord Howe Rise (Tilburg *et al.*, 2001). A considerable amount of the flow does not penetrate the northern constricted part of the basin thus potentially limiting the northern extension of the temperate bottom fauna. However, this does not explain the presence of tropical abyssal species in the northern section of the basin. Most of these species are eurybathyal to some extent, thus it is not improbable that propagules (or adults pelagic species) can disperse through the northern Cato Trough (min depth ~3100 m), or even across deeper sections of the northern Lord Howe Rise, forming a continuous fauna with abyssal basins to the north and east (Fig. 6).

The abyssal fauna could be affected by environmental change in surface waters via a vertical migration of larvae. Planktotrophic larvae of some deep-sea species have been recorded from surface waters (Gage and Tyler, 1991), where they presumably feed on available phytoplankton. Lecithotrophy is a more common life developmental strategy for LBA animals and some positively-buoyant yolky propagules have been found to migrate vertically (Gage and Tyler, 1991). Metamorphosed juveniles of several lecithotrophic elasipod holothurians have been found kilometres off the seafloor in the NE Atlantic Ocean (Gage and Tyler, 1991).

Unravelling the underlying causes of the LBA temperate-tropical transition will require additional descriptive and experimental studies. It would seem profitable to focus on the processes that potentially link LBA communities to the strong latitudinal environmental gradients that occur in shallower waters. The heterotrophic LBA deep sea is heavily dependent on quantity and type of organic inputs from the surface waters including carcass falls. The upper water column is the medium through which, at least some, species disperse and recruit. Finally, biotic interactions with regionally specific pelagic faunas (e.g. via predation from regionally restricted species) could also influence community composition.

The implication for management is that biodiversity at lower bathyal and abyssal depths is not uniform. Marine parks designs need to incorporate major biogeographic transitions such as the one shown in this study. Fortunately, Australia's newly declared marine park system (see https://parksaustralia.gov.au/marine/) includes seven reserves spaced along the eastern continental margin, although they are grouped into three networks (SE Australia, Temperate Eastern Australia and the Coral Sea) that do not reflect the distribution of the deep-sea fauna faunas identified here.

5. Conclusions

The benthic megafauna off the lower eastern Australian continental margin is structured primarily by depth strata and then region (northern vs southern). Thus the temperate-tropical transition, well known from shallow water environments, extends to the abyssal plain. This is noteworthy as the factors associated with shallow water biogeography, such as temperature and salinity, are relatively consistent for each depth layer across our study area. However, carbon flux to the seafloor does vary with both latitude and depth and may be the cause of varying assemblage composition of these heterotrophic systems. Alternatively, the benthic assemblages may be linked to the more structured environment of the upper ocean through larval dispersal or biotic interactions. The deep-sea is not a uniform environment and assemblage composition differs at regional scales, a pattern that needs to be integrated into spatial management of our oceans.

Supplementary Material

The supplementary material consists of a spreadsheet with the following worksheets: (S1) Taxonomic group abundances (counts), as counted on-board ship. (S2) Taxonomic group biomass (g), as weighed on-board ship. (S3) R scripts used for SpeciesMix and multivariate analyses and graphs. (S4) Species-sample abundance matrix (for species occurring in >= 2 samples). (S5) Sample environmental factors. (S6) Species-sample accumulation. (S7) Beta diversity decomposition. (S8) Forward selection of model parameters. (S9) Archetype standard errors for depth-latitude prediction landscape. (S10) Archetype fit graphed against temperature and POC flux. (S11) Species archetype tau predictions (probability of a species occurring in each archetype). (S12) Distributional range information for species that are part of the N4000 archetype.

Acknowledgements

The authors wish to thank the CSIRO Marine National Facility (MNF) for its support in the form of sea time on RV Investigator, support personnel, scientific equipment and data management. All data and samples acquired on the voyage are made publically available in accordance with MNF Policy. We also thank all the scientific staff and crew who participated in voyage IN2017_V03. Project funding was provided by the Marine Biodiversity Hub, supported through the Australian Government's National Environmental Science Program (NESP). The following taxonomists provided specimen identifications: Merricks Ekins and Ella Lejeune (QM, Porifera & Tunicata), Andrea Crowther (SAM, Actiniaria), Michela Mitchell (MV, Actiniaria), Hiroki Kise (University of the Ryukyus, Zoantharia), Phil Alderslade and Candice Untiedt (CSIRO, Octocorallia), Kirrily Moore (TMAG, Octocorallia), Robin Wilson (MV, Annelida), Elena Kupriyanova, Laetitia Gunton, Pat Hutchings, Anna Murray, Jinghuai Zhang and Hannelore Paxton (AM, Annelida), Caroline Farrelly (MV, Decapoda), Shane Ahyong (AM, Decapoda), Andrew Hosie (WAM, Cirripedia), David Staples (MV, Pycnogonida), Hugh McIntosh (MV, Bivalvia), Frank Köhler, Francesco Criscione and Anders Hallan (AM, Gastropoda), Julian Finn and C.C. Lu (MV, Cephalopoda), Marc Eléaume (MNHN, Crinoidea), Christopher Mah (NMNH, Asteroidea), Tim O'Hara (MV, Ophiuroidea), Ashley Miskelly (AM, Echinoidea), Mark O'Loughlin and Melanie Mackenzie (MV, Holothuroidea), Martin Gomon and Di Bray (MV, Pisces), John Pogonoski and Alistair Graham (CSIRO, Pisces). The photograph of the Faceless Cusk (Fig. 3d) was taken by Rob Zugaro, MV. The material was lawfully collected under the following permits: (1) Access to Biological Resources in a Commonwealth Area for Non-Commercial Purposes, AU-COM2017-352; (2) Approval

for Activity in a Commonwealth Marine Reserve, CMR-17-000455; (3) Australian Fisheries Management Authority Scientific Permit, 1003393; (4) Queensland Government General Fisheries Permit, 191670; (5) Museums Victoria Animal Ethics Committee approval, MV AEC 17001.

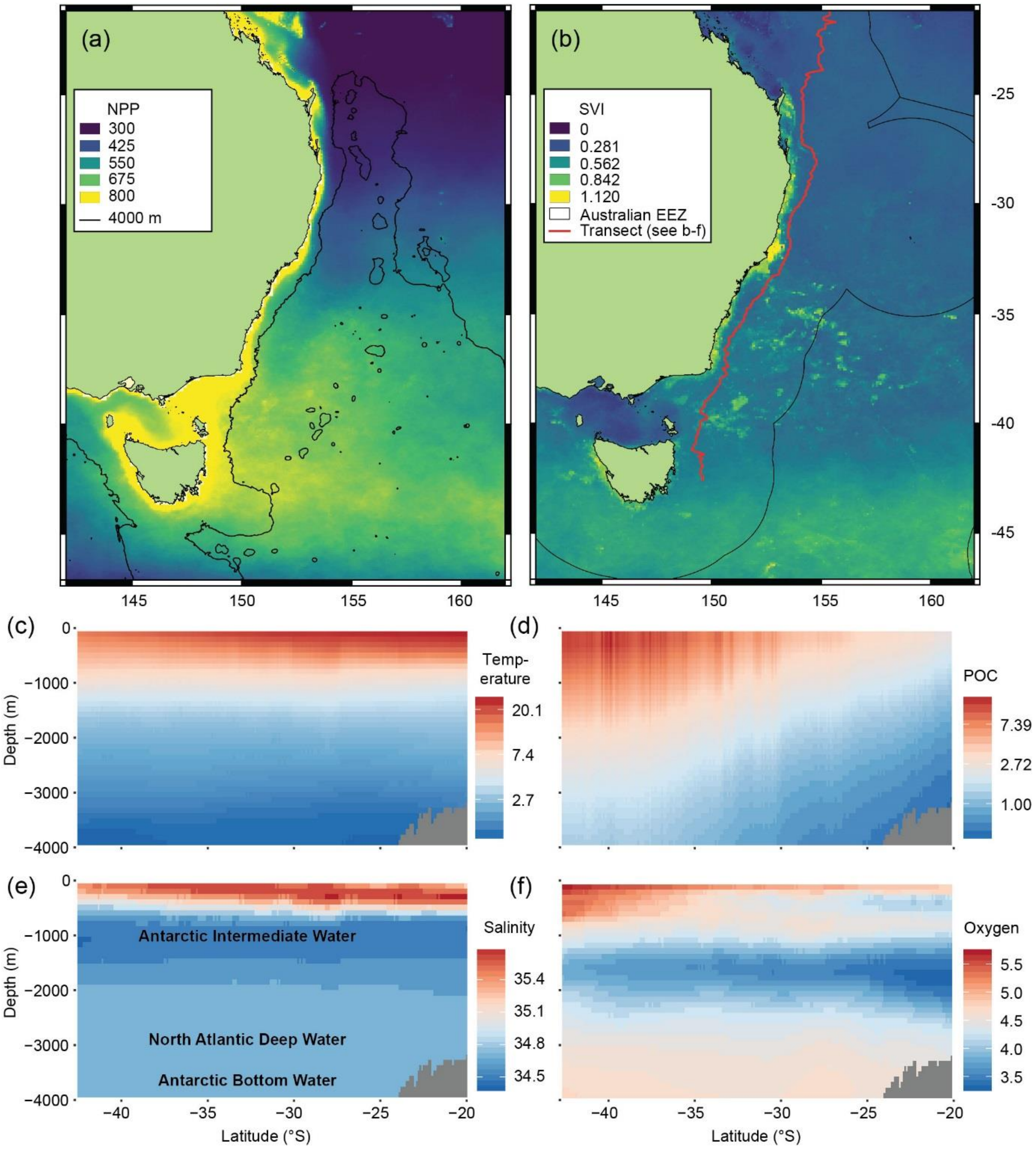

Fig. 1. (a) Net Primary Production (NPP; g C_{org} m^{-2} yr^{-1}) derived from a vertically generalized production model (VGPM) from satellite-derived chlorophyll (see methods). (b) Seasonal Variation Index of NPP (SVI). (c) Sea temperature (°C) interpolated from the CARS2009 dataset. (d) Particulate organic matter flux to depth (POC; g C_{org} m^{-2} yr^{-1}) calculated using the regression equation of Lutz et al. (2007). (e) Salinity (‰) and (f) Oxygen concentration (ml/l) interpolated from the CARS2009 dataset. The transect used to generate the depth-latitude plots (c-f), indicated in red on (b), follows

the 4000 m contour north until ~24S after which it enters the Cato Trough (indicated in grey on the lower right corner of c-f). The colour schemes in (c-d) are set to a log scale to emphasise latitudinal variation across depth layers.

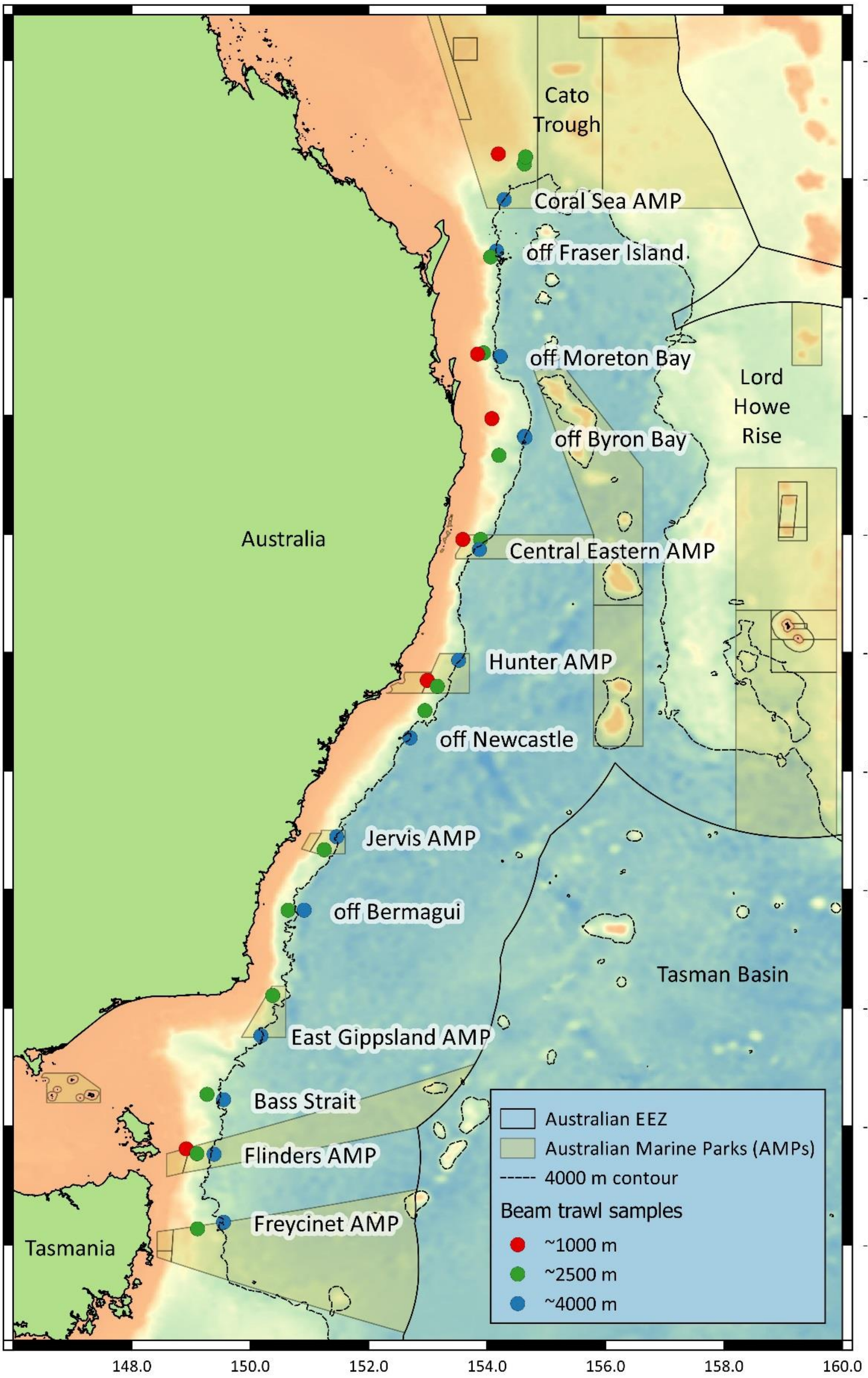

Fig. 2. Map of the eastern Australian continental margin showing sample sites. Note the lateral constriction of the Tasman Basin, at 4000 m water depth, north of Newcastle.

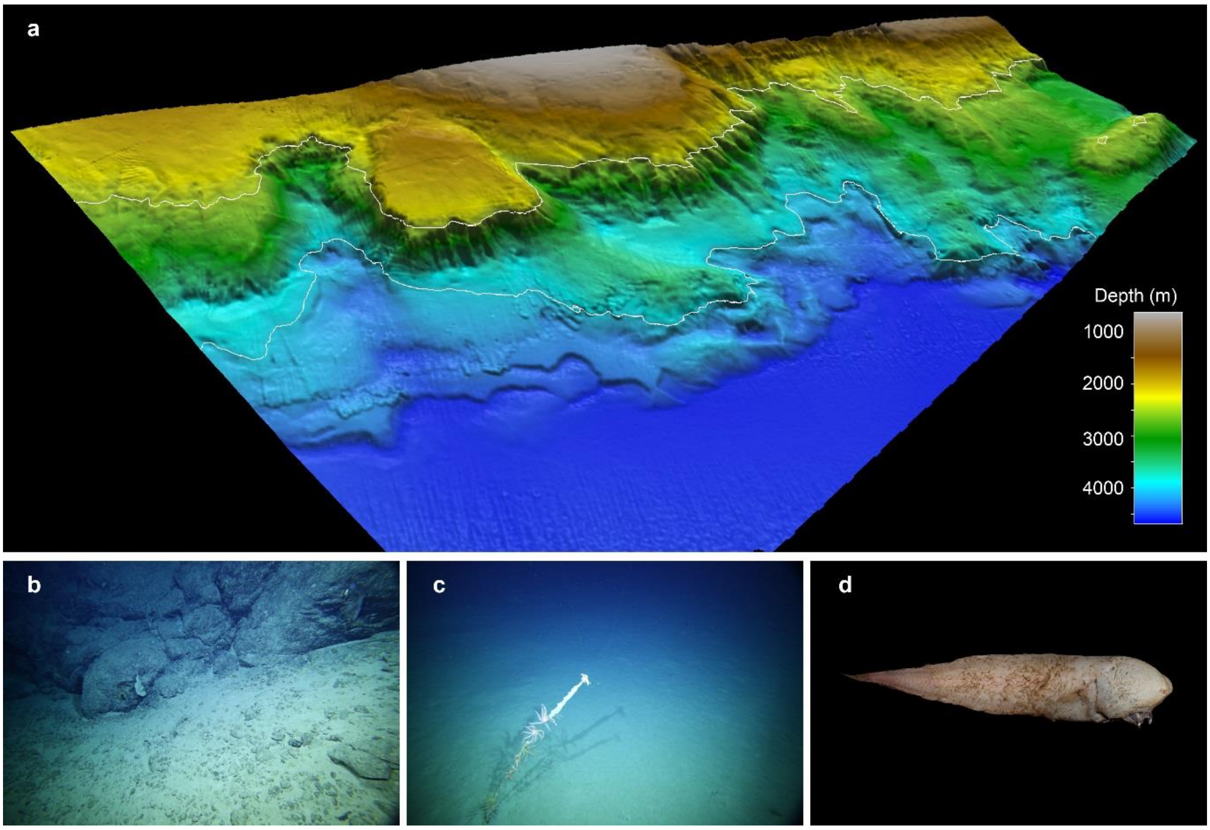

Fig. 3. (a) 3D bathymetric image of East Gippsland AMP (see Fig. 2), showing the mostly rugged topography of the seabed along the 2500 and 4000 m depth contours (white lines). The IN2017_V03 voyage mapped this marine park at high resolution for the first time. (b) Image of a rocky outcrop at ~1800 m from the Hunter AMP. (c) Sea-whip covered in crinoids at ~1900 m on a sediment plain in the Central Eastern AMP. (d) The Faceless Cusk Fish (*Typhlonus nasus*) from beam trawl 053 off Jervis Bay (photo: Rob Zugaro, MV).

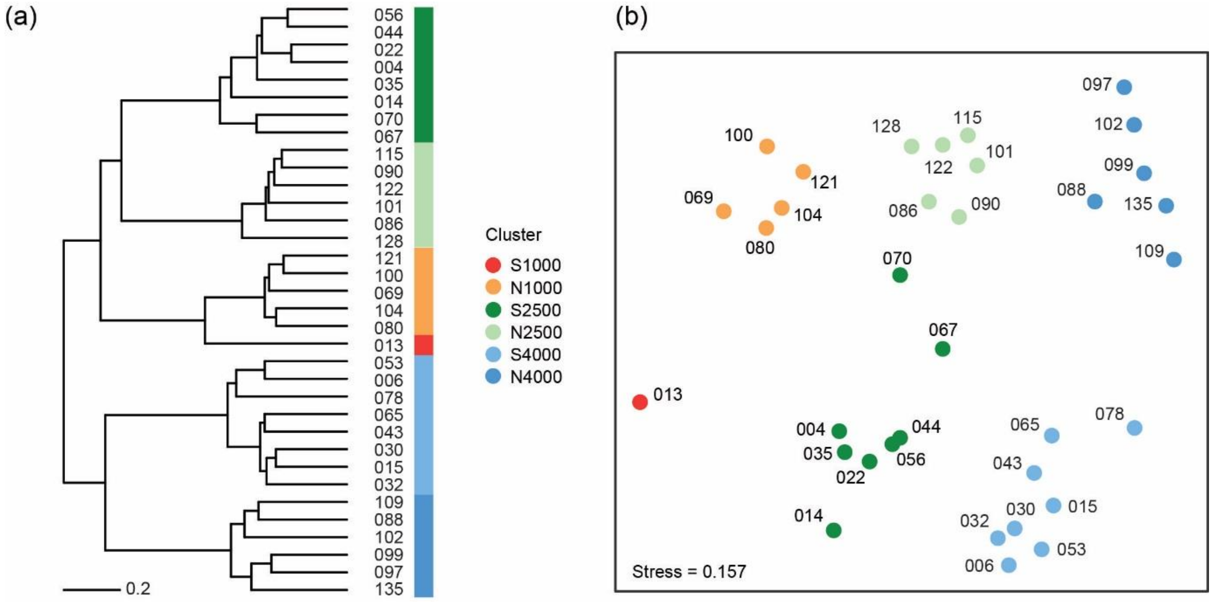

Fig. 4. Non-metric hierarchical clustering and ordination (nMDS) of sample data showing the samples clustered into 6 groups, based on southern temperate (S) and northern tropical (N) locations and target sample depths (1000, 2500 and 4000 m).

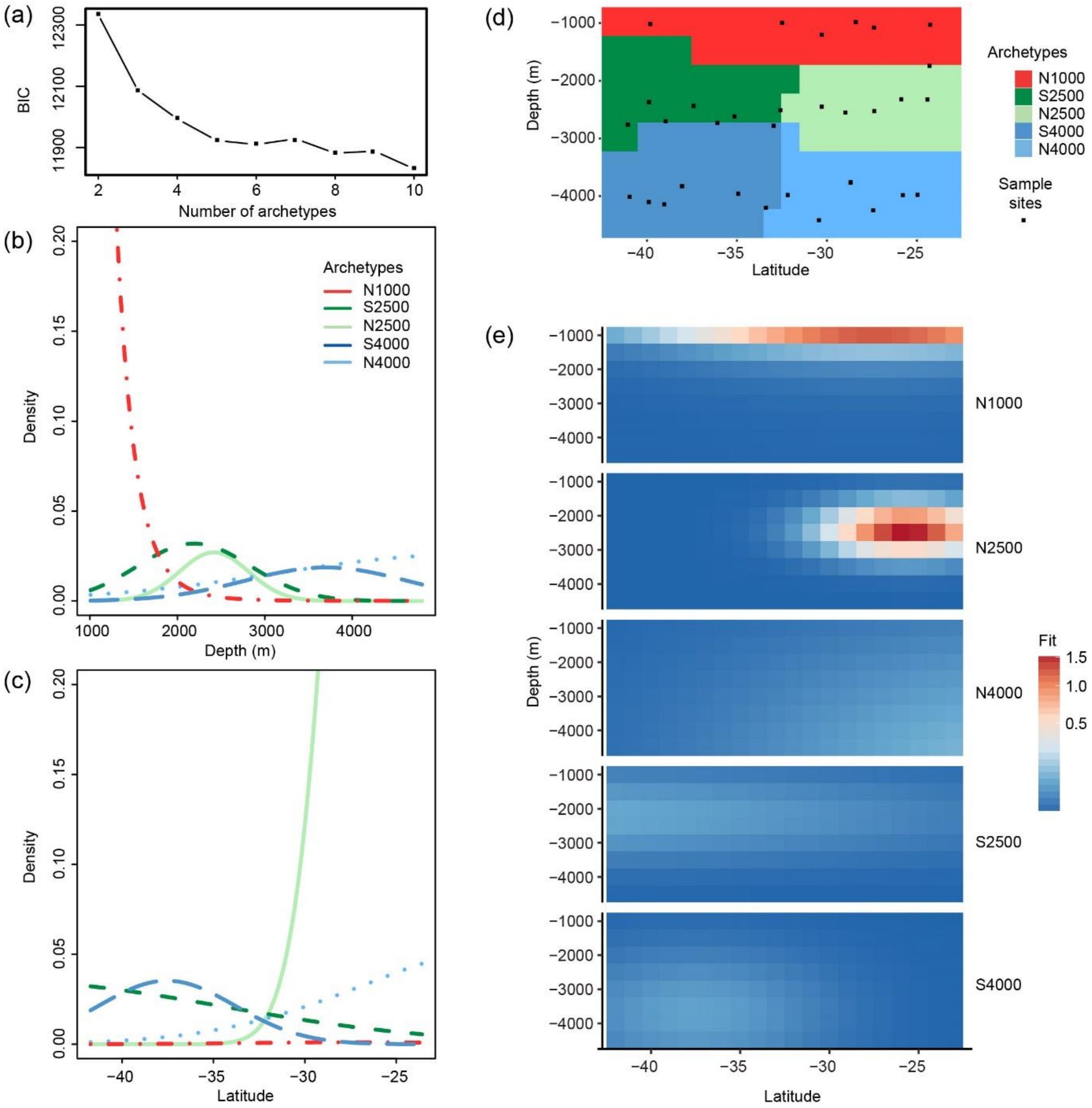

Fig. 5. SpeciesMix model-based analysis to delimit species archetypes. (a) BIC results level off after five clusters which correspond to the N1000, S2500, N2500, S4000 and N4000 groups identified in Fig. 3. (b-c) Responses of the environmental factors, sample depth and latitude, to each archetype. (d) Archetypes with the greatest predicted density (tau) mapped across depth and latitude (500 m x 1° cells). (e) Archetype specific predictions showing the overlap between southern (S) and northern (N) groups at each depth range.

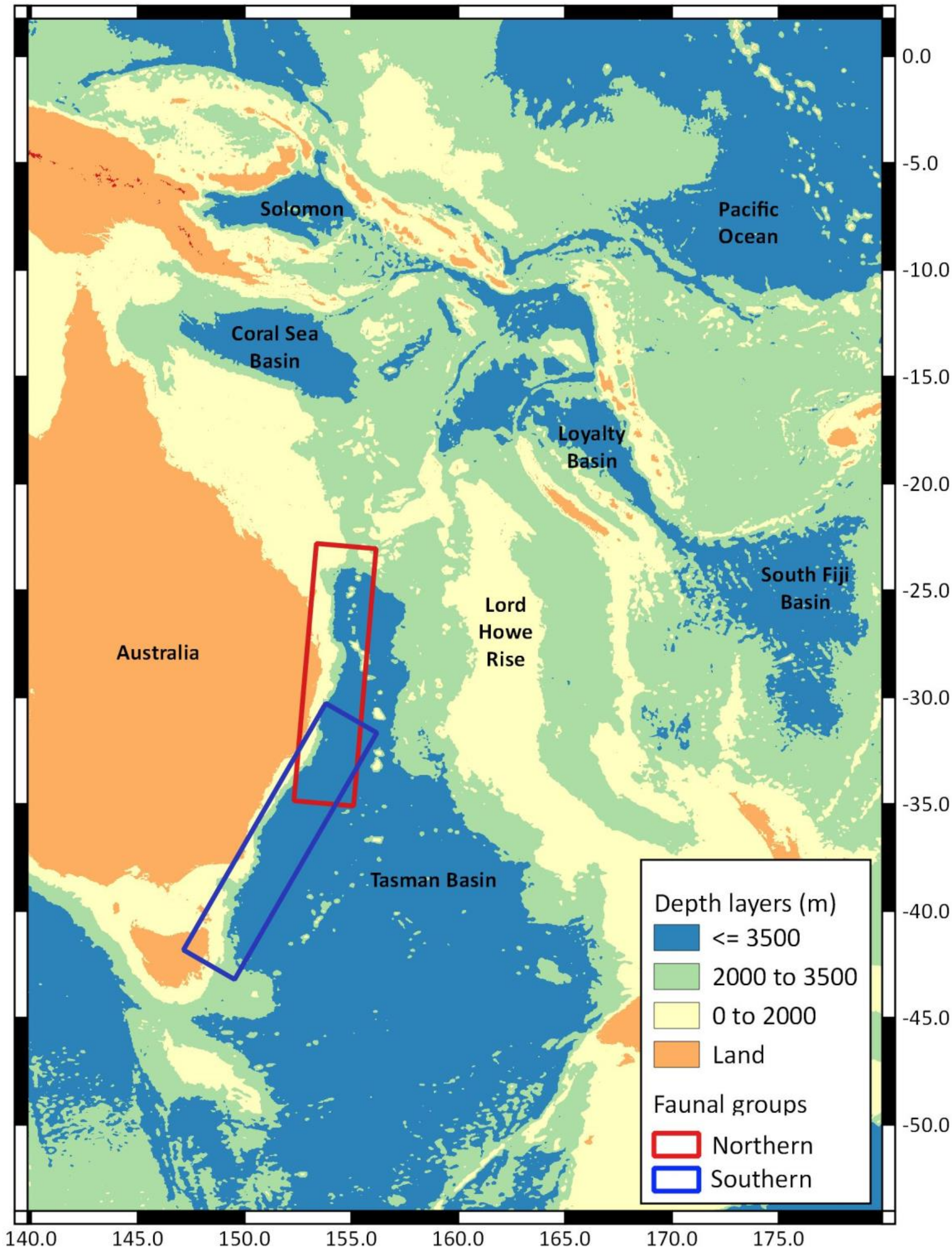

Fig. 6. Map of abyssal basins in the south-west Pacific Ocean, showing the location of northern and southern faunal groups observed in this study.

,

Stn	Location	Latitude	Longitude	Mid depth (m)	Date (d/m/y)	Biomass (g)	Abundance	Area sampled (m^2)	Adj. biomass (g)	Adj. abund.	Temp. (°C)	Salinity (‰)	POC (g $m^{-2}y^{-1}$)	Site cluster	Archetype
004	Freycinet MP	-41.731	149.120	2785	18/5/17	72138	2027	29584	2438	69	1.7537	34.7291	1.998	S2500	S2500
006	Freycinet MP	-41.626	149.552	4037	18/5/17	538	238	30344	18	8	1.0775	34.7074	1.260	S4000	S4000
013	Flinders MP	-40.386	148.928	1041	20/5/17	403	84	7908	51	11	4.4411	34.4686	6.166	S1000	1000
014	Flinders MP	-40.464	149.102	2392	20/5/17	8115	189	15348	529	12	1.9578	34.7166	2.352	S2500	S2500
015	Flinders MP	-40.473	149.397	4126	20/5/17	1306	593	10572	124	56	1.1405	34.7036	1.198	S4000	S4000
022	Bass Strait	-39.462	149.276	2726	22/5/17	15958	2478	11756	1357	211	1.7794	34.7213	2.049	S2500	S2500
030	Bass Strait	-39.552	149.553	4165	23/5/17	896	402	29312	31	14	1.0396	34.6974	1.181	S4000	S4000
032	East Gippsland MP	-38.479	150.184	3851	24/5/17	2235	468	11580	193	40	1.1299	34.7040	1.290	S4000	S4000
035	East Gippsland MP	-37.792	150.382	2459	25/5/17	7503	698	15352	489	45	1.8944	34.7072	2.264	S2500	S2500
043	Off Bermagui	-36.351	150.914	4800	27/5/17	608	328	14824	41	22	1.1793	34.7013	0.959	S4000	S4000
044	Off Bermagui	-36.355	150.644	2754	27/5/17	7486	1190	17972	417	66	1.7226	34.6805	1.726	S2500	S2500
053	Jervis MP	-35.114	151.469	3981	28/5/17	1650	140	16792	98	8	1.2244	34.7038	1.045	S4000	S4000
056	Jervis MP	-35.333	151.258	2643	29/5/17	9466	3523	15976	593	221	1.7508	34.7118	1.657	S2500	S2500
065	Off Newcastle	-33.441	152.702	4226	30/5/17	817	461	13992	58	33	1.1952	34.7011	0.847	S4000	S4000
067	Off Newcastle	-32.985	152.952	2803	31/5/17	6486	290	19748	328	15	1.8818	34.7039	1.274	S2500	N2500
069	Hunter MP	-32.479	152.994	1021	3/6/17	6478	1900	12508	518	152	5.4223	34.4436	5.352	N1000	1000
070	Hunter MP	-32.575	153.162	2534	3/6/17	8433	715	26260	321	27	1.9117	34.7039	1.405	S2500	N2500
078	Hunter MP	-32.138	153.527	4004	4/6/17	438	79	19608	22	4	1.1873	34.6993	0.793	S4000	N4000
080	Central Eastern MP	-30.099	153.596	1225	5/6/17	16053	1236	16096	997	77	4.2400	34.4640	3.471	N1000	1000
086	Central Eastern MP	-30.098	153.899	2473	5/6/17	2379	373	13384	178	28	2.0119	34.6929	1.193	N2500	N2500
088	Central Eastern MP	-30.264	153.870	4441	6/6/17	1055	377	18328	58	21	1.1856	34.6954	0.687	N4000	N4000
090	Off Byron Bay	-28.677	154.203	2574	7/6/17	4024	412	15400	261	27	1.8375	34.6998	0.981	N2500	N2500
097	Off Byron Bay	-28.355	154.636	3782	8/6/17	1635	279	27508	59	10	1.1552	34.6980	0.646	N4000	N4000
099	Off Byron Bay	-28.371	154.649	3789	9/6/17	1448	646	14416	100	45	1.1550	34.6979	0.646	N4000	N4000
100	Off Byron Bay	-28.054	154.083	1006	9/6/17	27174	1497	18968	1433	79	5.0321	34.4412	2.369	N1000	1000
101	Off Moreton Bay	-26.946	153.945	2548	9/6/17	262	216	11564	23	19	1.9569	34.6972	1.017	N2500	N2500
102	Off Moreton Bay	-27.008	154.223	4269	10/6/17	1049	220	18332	57	12	1.1909	34.6976	0.575	N4000	N4000
104	Off Moreton Bay	-26.961	153.848	1104	10/6/17	3438	603	13352	257	45	4.4712	34.4483	2.411	N1000	1000
109	Off Fraser Island	-25.221	154.164	4005	11/6/17	1744	104	18156	96	6	1.1585	34.6972	0.542	N4000	N4000
115	Off Fraser Island	-25.325	154.068	2346	11/6/17	2213	1274	11976	185	106	2.1208	34.6780	0.905	N2500	N2500
121	Coral Sea MP	-23.587	154.194	1053	13/6/17	5809	763	13352	435	57	4.5996	34.4645	1.674	N1000	1000
122	Coral Sea MP	-23.751	154.639	2349	13/6/17	794	289	13548	59	21	2.0107	34.6884	0.816	N2500	N2500
128	Coral Sea MP	-23.631	154.660	1765	13/6/17	4740	1911	13964	339	137	2.5708	34.6170	1.086	N2500	N2500
135	Coral Sea MP	-24.352	154.291	4001	15/6/17	51	28	19812	3	1	1.1436	34.6996	0.517	N4000	N4000

Table 1. Sample location and environmental data, predicted clusters and archetypes. Adj = adjusted by area of sample.

References

Baselga, A., 2010. Partitioning the turnover and nestedness components of beta diversity. Global Ecology and Biogeography 19, 134-143.

Baselga, A., Orme, D., Villeger, S., De Bortoli, J., Leprieur, F., 2018. betapart: Partitioning Beta Diversity into Turnover and Nestedness Components. R package version 1.5.1. https://CRAN.R-project.org/package=betapart.

Behrenfeld, M.J., Falkowski, P.G., 1997. Photosynthetic rates derived from satellite-based chlorophyll concentration. Limnology and Oceanography 42, 1-20.

Behrenfeld, M.J., O'Malley, R.T., Siegel, D.A., McClain, C.R., Sarmiento, J.L., Feldman, G.C., Milligan, A.J., Falkowski, P.G., Letelier, R.M., Boss, E.S., 2006. Climate-driven trends in contemporary ocean productivity. Nature 444 (7120), 752-755.

Carney, R.S., 2005. Zonation of deep biota on continental margins. Oceanography and Marine Biology: An Annual Review 43, 211-278.

Chiswell, S.M., Bostock, H.C., Sutton, P.J.H., Williams, M.J.M., 2015. Physical oceanography of the deep seas around New Zealand: a review. New Zealand Journal of Marine and Freshwater Research 49 (2), 286-317.

Clarke, K.R., Warwick, R.M., 2001. Change in marine communities: An approach to statistical analysis and interpretation. 2nd Edition. Natural Environment Research Council and Plymouth Marine Laboratory, UK.

Condie, S., 1994. A circulation model of the abyssal Tasman Sea. Deep Sea Research Part I: Oceanographic Research Papers 41 (1), 9-22.

Crame, J.A., 2018. Key stages in the evolution of the Antarctic marine fauna. Journal of Biogeography 45 (5), 986-994.

Crossingham, T.J., Vasconcelos, P.M., Cunningham, T., Knesel, K.M., 2017. 40Ar/39Ar geochronology and volume estimates of the Tasmantid Seamounts: Support for a change in the motion of the Australian plate. Journal of Volcanology and Geothermal Research 343, 95-108.

Danovaro, R., Snelgrove, P.V.R., Tyler, P., 2014. Challenging the paradigms of deep-sea ecology. Trends in Ecology and Evolution 29 (8), 465-475.

Dunstan, P.K., Foster, S.D., Darnell, R., 2011. Model based grouping of species across environmental gradients. Ecological Modelling 222, 955–963.

Dunstan, P.K., Foster, S.D., Hui, F.K.C., Warton, D.I., 2013. Finite Mixture of Regression Modeling for High-Dimensional Count and Biomass Data in Ecology. Journal of Agricultural, Biological, and Environmental Statistics 18 (3), 357-375.

Ekman, S., 1953. The Zoogeography of the Sea. Sidgwick and Jackson Ltd, London.

Falkowski, P.G., Algeo, T., Codispoti, L., Deutsch, C., Emerson, S., Hales, B., Huey, R.B., Jenkins, W.J., Kump, L.R., Levin, L.A., Lyons, T.W., Nelson, N.B., Schofield, O.S., Summons, R., Talley, L.D., Thomas, E., Whitney, F., Pilcher, C.B., 2011. Ocean deoxygenation: Past, present, and future. Eos, Transactions American Geophysical Union 92 (46), 409-410.

Fine, P.V.A., 2015. Ecological and Evolutionary Drivers of Geographic Variation in Species Diversity. Annual Review of Ecology, Evolution, and Systematics 46 (1), 369-392.

Gage, J.D., Tyler, P.A., 1991. Deep sea biology: A natural history of organisms at the deep-sea floor. Cambridge University Press, Cambridge.

Gaina, C., Müller, D.R., Royer, J.-Y., Stock, J., Hardebeck, J., Symonds, P., 1998. The tectonic history of the Tasman Sea: A puzzle with 13 pieces. Journal of Geophysical Research 103 (B6), 12413-12433.

Hallegraeff, G.M., Richardson, A.J., Coughlan, A., 2017. Chapter 3: Marine Phytoplankton Bioregions in Australian Seas. In: Ebach, M.C. (Ed.), Handbook of Australasian Biogeography. CRC Press, Boca Raton, pp. 1-12.

Heap, A.D., Harris, P.T., 2008. Geomorphology of the Australian margin and adjacent seafloor. Australian Journal of Earth Sciences 55 (4), 555-585.

Henschke, N., Everett, J.D., Richardson, A.J., Suthers, I.M., 2016. Rethinking the Role of Salps in the Ocean. Trends in Ecology and Evolution 31 (9), 720-733.

Henson, S.A., Dunne, J.P., Sarmiento, J.L., 2009. Decadal variability in North Atlantic phytoplankton blooms. Journal of Geophysical Research: Oceans 114 (C4).

Hidas, E.Z., Costa, T.L., Ayre, D.J., Minchinton, T.E., 2007. Is the species composition of rocky intertidal invertebrates across a biogeographic barrier in south-eastern Australia related to their potential for dispersal? Marine and Freshwater Research 58 (9), 835-842.

Hubble, T., Yu, P., Airey, D., Clarke, S., Boyd, R., Keene, J., Exon, N., Gardner, J., 2012. Physical Properties and Age of Continental Slope Sediments Dredged from the Eastern Australian Continental Margin – Implications for Timing of Slope Failure. In: Yamada, Y., Kawamura, K., Ikehara, K., Ogawa, Y., Urgeles, R., Mosher, D., Chaytor, J., Strasser, M. (Eds.), Submarine Mass Movements and Their Consequences. Advances in Natural and Technological Hazards Research, vol 31. Springer, Dordrecht, pp. 43-54.

Johnston, A.K., 1856. The Physical Atlas Of Natural Phenomena. A New Enlarged Edition. William Blackwood & Sons, London

Keene, J., Baker, C., Tran, M., Potter, A., 2008. Geomorphology and Sedimentology of the East Marine Region of Australia. Geoscience Australia, Record 2008/10. Geoscience Australia, Canberra.

Last, P.R., Lyne, V.D., Williams, A., Davies, C.R., Butler, A.J., Yearsley, G.K., 2010. A hierarchical framework for classifying seabed biodiversity with application to planning and managing Australia’s marine biological resources. Biological Conservation 143, 1675–1686.

Lutz, M., Dunbar, R., Caldeira, K., 2002. Regional variability in the vertical flux of particulate organic carbon in the ocean interior. Global Biogeochemical Cycles 16 (3), 11 (11-18).

Lutz, M.J., Caldeira, K., Dunbar, R.B., Behrenfeld, M.J., 2007. Seasonal rhythms of net primary production and particulate organic carbon flux describe biological pump efficiency in the global ocean. Journal of Geophysical Research 112, C10011.

MacArthur, R.H., Wilson, E.O., 1967. The theory of island biogeography. Princeton University Press, Princeton, N.J.

Madsen, F.J., 1961. On the zoogeography and origin of the abyssal fauna in view of knowledge of the Porcellanasteridae. Galathea Report 4, 177-218.

Martinez, I.J., 1994. Late Pleistocene carbonate dissolution patterns in the Tasman Sea. In: van der Lingen, G.J., Swanson, K., Muir, R.J. (Eds.), Evolution of the Tasman Sea Basin. Balkema, Rotterdam, pp. 215-228.

Menzies, R.J., George, R.Y., Rowe, G.T., 1973. Abyssal environment and ecology of the world oceans. Wiley-Interscience, New York and London.

Murray, J., 1895. A summary of the scientific results. I-II. Report on the Scientific Results of the Voyage of H.M.S. Challenger during the Years 1872-76, xix + 1608 pp, 1622 plates.

O'Hara, T.D., Hugall, A.F., Woolley, S.N.C., Bribiesca-Contreras, G., Bax, N.J., 2019. Contrasting processes drive ophiuroid phylodiversity across shallow and deep seafloors. Nature 565 (7741), 636–639.

O'Hara, T.D., Rowden, A.A., Bax, N.J., 2011. A southern hemisphere bathyal fauna is distributed in latitudinal bands. Current Biology 21, 226-230.

O’Hara, R.B., Kotze, D.J., 2010. Do not log-transform count data. Methods in Ecology and Evolution 1 (2), 118-122.

Oksanen, J., Blanchet, F.G., Kindt, R., Legendre, P., Minchin, P.R., O'Hara, R.B., Simpson, G.L., Solymos, P., Stevens, M.H.H., Wagner, H., 2016. vegan: Community Ecology Package. R package version 2.3-5. http://CRAN.R-project.org/package=vegan.

R Core Team, 2017. R: A language and environment for statistical computing. R Foundation for Statistical Computing, Vienna, Austria.

Raes, E.J., Bodrossy, L., van de Kamp, J., Bissett, A., Ostrowski, M., Brown, M.V., Sow, S.L.S., Sloyan, B., Waite, A.M., 2018. Oceanographic boundaries constrain microbial diversity gradients in the South Pacific Ocean. Proceedings of the National Academy of Sciences 115 (35), E8266-E8275.

Ridgway, K.R., Dunn, J.R., 2003. Mesoscale structure of the mean East Australian Current System and its relationship with topography. Progress in Oceanography 56, 189–222.

Ridgway, K.R., Dunn, J.R., Wilkin, J.L., 2002. Ocean interpolation by four-dimensional least squares - Application to the waters around Australia. Journal of Atmospheric and Oceanic Technology 19, 1357-1375.

Schnabel, K.E., Cabezas, P., McCallum, A., Macpherson, E., Ahyong, S., Baba, K., 2011. Worldwide patters of distribution of squat lobsters (Galatheidae and Chirostylidae: Anomura). In: Poore, G.C.B., Ahyong, S.T., Taylor, J. (Eds.), Squat Lobster Biology. CSIRO Publishing, Melbourne, pp. 149-182.

Seiter, K., Hensen, C., Schroter, J., Zabel, M., 2004. Organic carbon content in surface sediments – defining regional provinces. Deep Sea Research Part I: Oceanographic Research Papers 51, 2001–2026.

Smith, C.R., Baco, A.R., 2003. Ecology of whale falls at the deep-sea floor. Oceanography and Marine Biology: An Annual Review 41, 311–354.

Smith, K.L., Jr., Ruhl, H.A., Bett, B.J., Billett, D.S.M., Lampitt, R.S., Kaufmann, R.S., 2009. Climate, carbon cycling, and deep-ocean ecosystems. Proceedings of the National Academy of Sciences of the United States of America 106 (46), 19211-19218.

Stuart-Smith, R.D., Edgar, G.J., Bates, A.E., 2017. Thermal limits to the geographic distributions of shallow-water marine species. Nature Ecology & Evolution 1 (12), 1846-1852.

Thuy, B., Gale, A.S., Kroh, A., Kucera, M., Numberger-Thuy, L.D., Reich, M., Stöhr, S., 2012. Ancient origin of the modern deep-sea fauna. PLoS ONE 7 (10), e46913.

Tilburg, C.E., Hurlburt, H.E., O'Brien, J.J., Shriver, J.F., 2001. The Dynamics of the East Australian Current System: The Tasman Front, the East Auckland Current, and the East Cape Current. Journal of Physical Oceanography 31, 2917-2943.

Tomczak, M., Godfrey, J.S., 2003. Regional Oceanography: An Introduction. Daya Publishing House, Delhi.

UNESCO, 2009. Global Open Oceans and Deep Seabed (GOODS) – Biogeographic Classification. IOC Technical Series, 84. UNESCO-IOC., Paris.

Vinogradova, N.G., 1959. The zoogeographical distribution of the deep-water bottom fauna in the abyssal zone in the ocean. Deep Sea Research 5, 205-208.

Warton, D.I., Foster, S.D., De’ath, G., Stoklosa, J., Dunstan, P.K., 2015. Model-based thinking for community ecology. Plant Ecology 216 (5), 669-682.

Warton, D.I., Wright, S.T., Wang, Y., 2012. Distance-based multivariate analyses confound location and dispersion effects. Methods in Ecology and Evolution 3, 89-101.

Watling, L., Guinotte, J., Clark, M.R., Smith, C.R., 2013. A Proposed Biogeography of the Deep Ocean Floor. Progress in Oceanography 111, 91-112.

Wiens, J.J., Donoghue, M.J., 2004. Historical biogeography, ecology and species richness. Trends in Ecology and Evolution 19 (12), 639-644.

Williams, A., Althaus, F., Dunstan, P.K., Poore, G.C.B., Bax, N.J., Kloser, R.J., McEnnulty, F.R., 2010. Scales of habitat heterogeneity and megabenthos biodiversity on an extensive Australian continental margin (100-1,000m depths). Marine Ecology 31, 222-236.

Williams, A., Bax, N.J., Kloser, R.J., Althaus, F., Barker, B., Keith, G., 2009. Australia's deep-water reserve network: implications of false homogeneity for classifying abiotic surrogates of biodiversity. ICES Journal of Marine Science 66 (10), 214-224.

Wolff, G.A., Billett, D.S.M., Bett, B.J., Holtvoeth, J., FitzGeorge-Balfour, T., Fisher, E.H., Cross, I., Shannon, R., Salter, I., Boorman, B., King, N.J., Jamieson, A., Chaillan, F., 2011. The Effects of Natural Iron Fertilisation on Deep-Sea Ecology: The Crozet Plateau, Southern Indian Ocean. PLoS ONE 6 (6), e20697.

Woolley, S.N.C., Tittensor, D.P., Dunstan, P.K., Guillera-Arroita, G., Lahoz-Monfort, J.J., Wintle, B.A., Worm, B., O'Hara, T.D., 2016. Deep-sea diversity patterns are shaped by energy availability. Nature 533, 393–396.